Cage Compounds

DOI: 10.1002/anie.201104666

In-Between Complex and Cluster: A 14-Vertex Cage in $[Ag_2Se_{12}]^{2+}$**

*Tobias Köchner, Nils Trapp, Tobias A. Engesser, Anna J. Lehner, Caroline Röhr, Sebastian Riedel, Carsten Knapp, Harald Scherer, and Ingo Krossing**

Numerous cyclic sulfur and selenium allotropes E_n (E = S: n = 6–15, 18, 20 etc.; E = Se: n = 6, 7, 8) are known, while hexagonal Te_∞ remains the only accessible allotrope of tellurium.[1] For Se, the stability of the allotropes increases from $Se_7 < Se_6 < Se_8 < Se_\infty$. Although being structurally related to crown ethers, only a few examples of chalcogen rings coordinated to a metal ion exist, including $[Ag_n(Se_6)]^{n+}$ (n = 1, 2),[2,3] $[M(S_8)_n]^+$ (M = Cu;[4] Ag[5]), $[Cu(S_{12})]^+$, $[Cu(S_8)(S_{12})]^+$.[6] All of these cations are partnered with weakly coordinating anions (WCA).[7] Related salts containing almost non-interacting cationic stacks are $[Rb(Se_8)^+]_\infty$[8] and $[Rb(Se_6)_2^+]_\infty$.[9] The neutral selenium complexes $[PdX_2(Se_6)]$[10] (X = Cl, Br), $[(AgI)_2Se_6]$,[11] $[Re_2I_2(CO)_6(Se_7)]$,[12] and $[Rh_2(Se_9)Cl_6]$[13] complete this series.

Herein we are interested to discover, if in addition to metastable allotropes such as Se_6,[1] also hitherto unknown allotropes of selenium might be accessible by coordination to the silver ion. We reasoned that freshly prepared red amorphous selenium (metastable Se_6, Se_7, and Se_8 rings), should have a higher reactivity towards Ag[WCA] salts than the gray selenium, which led to Se_6 complexes.[2,3] Gray selenium and the vitreous red modification differ by $\Delta H^0 = 5\ kJ\,mol^{-1}$ and are separated by an activation energy of 115 kJ mol^{-1} (both values are per Se atom).[14,15]

Reactions of $Ag[Al(OR^F)_4]$ ($R^F = C(CF_3)_3$)[16] as well as the novel salt Ag[fal] ([fal] = $[FAl(OC(C_5F_{10})(C_6F_5))_3]$; see Supporting Information)[17] with red selenium yield salts of the $[Ag_2Se_{12}]^{2+}$ ion. Upon stirring or sonicating 1 equivalent of the silver salts and 6 equivalent of red, amorphous Se for several hours in 1,2-difluorobenzene (for Ag[fal]) or SO_2 (for $Ag[Al(OR^F)_4]$), the solutions turned to a deep orange color. Upon concentration and storage at 2 °C, orange crystals of $[Ag_2Se_{12}][fal]_2 \cdot 6\,C_6H_4F_2$ (**1**) that were only stable when kept in a 1,2-difluorobenzene atmosphere, formed from several batches. Small orange cubic crystals of $[Ag_2Se_{12}][Al(OR^F)_4]_2$ (**2**) were obtained from SO_2 in up to 81 % crystalline yield [Eq. (1)].

$$2\,Ag[A] + 12\,Se_{red} \rightarrow [Ag_2Se_{12}][A]_2 \qquad A = [fal]\ (\mathbf{1});\ [Al(OR^F)_4]\ (\mathbf{2}) \tag{1}$$

The solid-state standard reaction enthalpy for the formation of **2** from 12 equivalents Se_{red} and 2 equivalents of $Ag[Al(OR^F)_4]$ was examined in a suitable Born–Fajans–Haber cycle (see Supporting Information), and shown to be exothermic by −417 kJ mol^{-1}. This result suggests that Se_{12} formation in solid **2** was driven by thermodynamics. However, the signals in the ^{77}Se NMR spectra could not be unambiguously assigned to discrete species, but are consistent with a dynamic system that may involve equilibria and/or chemical exchange (see Supporting Information). Treating solutions of **2** with acetonitrile, immediately led to a red precipitate that probably contained larger amounts of Se_7 in addition to Se_6 and Se_8. The indications for forming Se_{12} were only indirect (see Supporting Information). Nevertheless, it appears that oligoselenium silver cations $[Ag_xSe_y]^{x+}$ are the dominant species in solution.

In contrast, the situation is clear in the solid state: Both structures include the D_{3d}-symmetric $[Ag_2Se_{12}]^{2+}$ ion which consists of a dodecaselenium ring formally complexed by two silver cations which in turn are in a trigonal-planar coordination environment. In **1**, $[Ag_2Se_{12}]^{2+}$ exhibits crystallographic C_i symmetry and the silver atoms have one strong contact to the (aluminum-bound) fluorine atoms of $[fal]^-$ enclosing the dication (Figure 1). $[Ag_2Se_{12}][Al(OR^F)_4]_2$ (**2**) containing the more symmetric anion, crystallizes in the trigonal space group $R\bar{3}m$ and consists of the crystallographically D_{3d}-symmetric $[Ag_2Se_{12}]^{2+}$ cation, surrounded by dis-

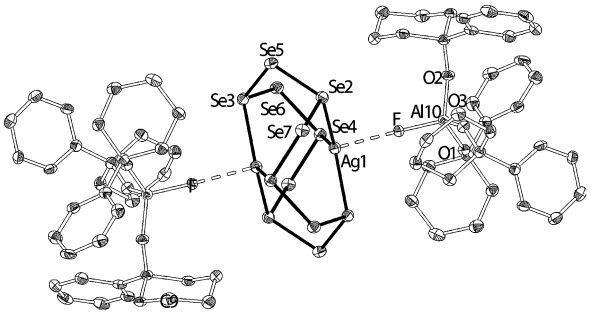

Figure 1. Section of the crystal lattice of $[Ag_2Se_{12}][fal]_2 \cdot 6\,C_6H_4F_2$. The solvent molecules as well as the fluorine atoms of the perfluorophenyl and perfluorohexyl ligands were omitted for clarity; thermal ellipsoids are set at 50 % probability. Selected bond lengths [pm]: Se2–Se7 233.53(8), Se2–Se5 234.17(8), Se2–Ag1 264.4(1), Se3–Se5 233.86(7), Se3–Se6 234.42(7), Se3–Ag1 264.6(1), Se4–Se6 233.6(1), Se4–Se7 234.14(7), Se4–Ag1 264.42(7), Ag1–F 242.0(2), Ag1–Ag1 297.1(1), Al10–F 169.2(2), Al10–O1 173.7(2), Al10–O2 174.0(2), Al10–O3 173.1(3).

[*] Dr. T. Köchner, Dr. N. Trapp, Dipl.-Chem. T. A. Engesser, Dipl.-Chem. A. J. Lehner, Prof. Dr.-Ing. C. Röhr, Dr. S. Riedel, Dr. C. Knapp, Dr. H. Scherer, Prof. Dr. I. Krossing
Institut für Anorganische und Analytische Chemie, Freiburger Materialforschungszentrum (FMF) and Freiburg Institute for Advanced Studies (FRIAS), Universität Freiburg
Albertstrasse 19, 79104 Freiburg (Germany)
E-mail: krossing@uni-freiburg.de

[**] This work was supported by the University of Freiburg and the Freiburg Institute of Advanced Studies FRIAS, Section Soft Matter Science.

Supporting information for this article is available on the WWW under http://dx.doi.org/10.1002/anie.201104666.

ordered $[Al(OR^F)_4]^-$ anions (see Supporting Information for discussion). The overall structure of the closed 14-vertex $[Ag_2Se_{12}]^{2+}$ cage formed by six six-membered rings in the boat conformation is unprecedented and a geometric description of this cage by means of Platonic or Archimedean polyhedra is not possible. Within the $[Ag_2Se_{12}]^{2+}$ dications (Figure 2), the puckered Se_{12} ring exhibits a similar conformation to S_{12},[18] and the two silver cations are in an almost trigonal planar

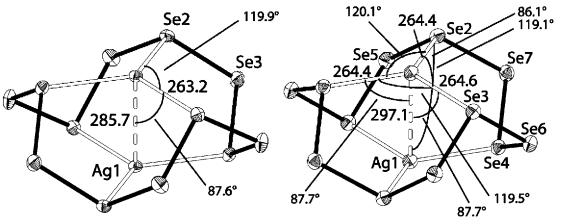

Figure 2. Molecular structure of the $[Ag_2Se_{12}]^{2+}$ dication in the solid-state structures of $[Ag_2Se_{12}][Al(OR^F)_4]_2$ (**2**, left) and $[Ag_2Se_{12}][fal]_2$ (**1**, right). Bond lengths [pm] and bond angles [°]. Thermal ellipsoids set at 50% probability. In **1**, d_{Se-Se} = 233.53(8)–234.42(7) pm and in **2**, d_{Se-Se} = 233.5(1)–233.6(1) pm.

environment (Σ(Se-Ag-Se) = 358.7° (**1**) and 359.5° (**2**)). The Ag–Ag distances of 297.10(1) (**1**) and 285.7(2) pm (**2**), respectively, are indicative for an argentophilic interaction (Σ(van der Waals (vdW) radii Ag): 344 pm).[14,19] In **1**, each silver atom is coordinated by one (Al-)fluorine with a Ag–F distance of 241.98(2) pm. This direct coordination of the $[fal]^-$ ion appears to be the main reason for the 11.4 pm elongation of the Ag–Ag distance compared with the isolated $[Al(OR^F)_4]^-$ structure. The average Se–Se distances of 233–234 pm are nearly equal for both structures and very similar to that in $(NH_4)_2[Mo_3S_{11.72}Se_{1.28}]\cdot[Se_{12}]$ (d_{Se-Se} = 232.7(2)–233.5(2) pm), which is the only other example of a Se_{12} ring.[20] The average Ag–Se distances decrease slightly from $[Ag_2Se_{12}][fal]_2$ (av.: 264.4 pm) to $[Ag_2Se_{12}][Al(OR^F)_4]_2$ (263.2 pm). This change may be attributed to stronger intracationic bonds in the noncoordinated cation, which leads to an overall contraction. The arrangement of the ions in the salt **2** follows a distorted CaF_2 type packing (radius-ratio rules: r_M/r_x = 0.86; see Supporting Information). Powder X-ray studies showed the bulk material to be also **2** (see Supporting Information). The ^{77}Se MAS NMR spectrum of **2** (see Supporting Information) has two pronounced resonances at δ = 1129 ppm and 756 ppm in agreement with the 2 × 6 equivalent Se nuclei in the structure. The anisotropy of the chemical shift is apparently higher for the up field signal and therefore we assign the δ = 1129 ppm signal to the selenium atoms next to silver. This assignment is in line with a significant deshielding effect on the positively polarized selenium atoms upon coordination to the silver ions. The signal at δ = 756 ppm then accounts for the remaining dicoordinate selenium atoms. Since all vibrational modes of $[Al(OR^F)_4]^-$ are well known,[21] a tentative assignment of the principle Se–Se mode in the IR spectrum was possible: In the diamond ATR (attenuated total reflection) spectrum (see Supporting Information) a medium intensity band at 202 cm^{-1} is assigned to a degenerate E_u scissoring mode of $[Ag_2Se_{12}]^{2+}$ (calculated with BP86/SVP: 200 cm^{-1}). Bands below 200 cm^{-1} could not be assigned with certainty and are omitted.[*]

Based on the selected PBE0/TZVPP model chemistry, the thermochemistry of the formation of the $[Ag_2Se_{12}]^{2+}$ unit was investigated in the gas phase, in solution (COSMO model[22]), as well as in the solid state (Table 1). For comparison, the energetic differences between Se_6, Se_8, and Se_{12} were also calculated with M052X/aug-cc-pVTZ-PP (see Table 1 a,b) that is known to deliver very accurate thermochemical values.[23] The calculated Gibbs energy difference between the rings Se_6, Se_8, and Se_{12} does not depend on the method and is less than 3 kJ mol^{-1} per Se atom in the gas phase; the most favored ring at room temperature is Se_8.

The formation of dissolved $[Ag_2Se_{12}]^{2+}$ (Table 1 c,d) is clearly favored and the alternative oxidation to the Se_8^{2+} dication (in Table 1 e) is disfavored by 89 to 125 kJ mol^{-1}. These investigations show that the formation of the otherwise only metastable Se_{12} ring in **2** is thermodynamically driven by complexation to the Ag^+ ions.

Table 1: Calculated reaction enthalpies and Gibbs energies: PBE0/TZVPP values are shown regular, BP86/SV(P) values in italics, the M052X/aug-cc-pVTZ-PP reference values in bold. Solvation corrections were calculated with the COSMO model (ε_r = 16.3, 298 K, SO_2; ε_r = 8.93, 298 K, CH_2Cl_2; ε_r = 13.59, 298 K, *o*-$C_6H_4F_2$).

Reaction	Δ_rH^{298}	Δ_rG^{298}	$\Delta_rG^{298}(SO_2)$	$\Delta_rG^{298}(CH_2Cl_2)$
a) $Se_{12} \rightarrow 2\,Se_6$	45/*54*/**43**	10/*18*/**8**		
b) $Se_{12} \rightarrow 1.5\,Se_8$	−4/−*14*/**6**	−18/−*27*/−**9**		
c) $2\,Ag^+ + Se_{12} \rightarrow [Ag_2Se_{12}]^{2+}$	−324/−*379*	−239/−*296*	−240/−*294*	−240
d) $Ag^+ + [AgSe_{12}]^+ \rightarrow [Ag_2Se_{12}]^{2+}$	17/−*3*	61/*39*	−77/−*98*	−66

Reaction	SM:[a]	Δ_rG^{298} (BFHC)[b] o-$C_6H_4F_2$	SO_2	CH_2Cl_2
e) $8\,Se_{(red)}\ (s) + 2\,Ag(SM)_3^+(solv) \rightarrow Se_8^{2+}(solv) + 2\,Ag^0(s) + 6\,SM$		+89	+104	+125

[a] SM: Solvent molecule. [b] BFHC = Born–Fajans–Haber cycle.

But to what extent is the charge in the $[Ag_2Se_{12}]^{2+}$ cage delocalized? Is the structure a coordination compound or a cluster? In this respect, both experimental crystal structures show Se–F and Ag–F contacts below the sum of vdW radii accounting for a recognizable charge delocalization on Se and Ag atoms (see Hirshfeld analysis in Figure 3, and the Supporting Information).

This result is in agreement with a PABOON population analysis: PABOON leads to a smooth charge delocalization over the selenium ring (Ag + 0.35; Se + 0.11/ + 0.11; Table 2).

[*] In the Raman spectrum more bands, for example, the intense A_{1g} symmetric stretching mode (244 cm^{-1} BP86/SVP), should be visible. Unfortunately, despite multiple attempts, a Raman spectrum could not be obtained as the compound fluoresces strongly. Several independent measurements between room temperature and −160 °C did not give utilizable spectra.

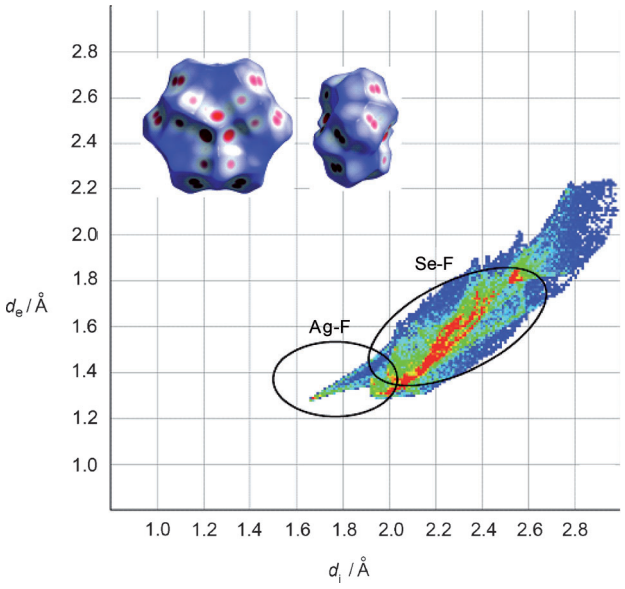

Figure 3. Projection of d_{norm} onto the Hirshfeld surface of the $[Ag_2Se_{12}]^{2+}$ dication in **2** calculated from the crystal structure: red areas account for distances shorter than the sum of the vdW radii, blue areas for distances longer than the sum of the vdW radii. Fingerprint plot for the $[Ag_2Se_{12}]^{2+}$ unit: d_e, distance from a point on the surface to the nearest nucleus outside the surface, d_i: distance from a point on the surface to the nearest nucleus in the surface. Red (many points with a d_e, d_i pair); blue (few points with a d_e, d_i pair); green and yellow (intermediate numbers of points with a d_e, d_i pair) Some characteristics of key intermolecular contacts are encircled.

In contrast, the NPA analysis localizes the charge more in the neighborhood of the Ag atom (+0.64 Ag; Se +0.11/−0.03). From the contact distribution in the solid state, it appears that PABOON offers a description closer to the experimental charge distribution (Figure 3).

But how are the bonds in the $[Ag_2Se_{12}]^{2+}$ cage formed? A natural bond orbital (NBO) population analysis on the dication assigns the Se–Se bonds as single bonds (Wiberg Bond Index (WBI) 0.99), while for the Ag–Se bonds a WBI of 0.29 and for the Ag–Ag interaction a WBI of 0.15 was calculated. The main donor–acceptor interactions assigned by the NBO analysis are donations of electron density from the three selenium lone pairs ($4p^2$ character) into the empty nonbonding orbitals of the neighboring silver cations ($5s^0$).

Table 2: Collected AIM results,[a] population analyses, and Wiberg bond indices.[b]

Data for the cage $[Ag_2Se_{12}]^{2+}$							
BCP	Bond	ρ(r) [e Å^{-3}][c]	ε(r)[c]	WBI	Atoms	PABOON	NPA
(3,-1)	Ag-Se	0.33	0.01	0.29	Ag	0.35	0.64
	Ag-Ag	0.16	0.00	0.15	$Se_{tricoord}$	0.11	0.15
	Se-Se	0.67	0.05	0.99	$Se_{dicoord}$	0.11	−0.03
(3,+1)	–	0.06	−1.20				

Data for free Se_{12}:	BCP	Bond	ρ(r) [e Å^{-3}]	ε(r)
	(3,-1)	Se-Se	0.72	0.01

[a] PBE0/def2-TZVPP(Se)/TZVPPalls2(Ag)//PBE0/def2-TZVPP(Se,Ag)). [b] PBE0/def2-TZVPP(Se,Ag). [c] ρ(r) = electron density residing on the CP; ε(r) = ellipticity in the CP.

This donated electron density again leads to significant donation into the Rydberg orbitals of the neighboring, weakly bound silver atom. The natural electron configuration of the Ag atoms in $[Ag_2Se_{12}]^{2+}$ ($5s^{0.37}4d^{9.94}5p^{0.03}6p^{0.01}$) suggests significant participation of the 5s orbitals in the Ag–Ag bond.

Atoms in molecules (AIM) calculations (Table 2) support the assignment of Ag–Ag bonding: a (3,−1) bond critical point (BCP) with an ellipticity of zero is located between the two silver atoms. The electron density at the BCP is small, but not negligible, with 0.16 e Å^{-3}. For the BCP on the Ag–Se bond the electron density is 0.33 e Å^{-3}, on the Se–Se BCP it is 0.67 e Å^{-3}. For comparison, the electron density residing on a Se–Se BCP in the free Se_{12} ring is 0.72 e Å^{-3}. This behavior accounts for the transfer of electron density towards silver. Moreover, six (3,+1) ring critical points (RCP) are formed, which surround the Ag–Ag BCP hexagonally (see Figure in Supporting Information).

To further verify the argentophilic interaction in the $[Ag_2Se_{12}]^{2+}$ dication, the PBE0/aug-cc-pVTZ optimized structure of $[Ag_2Se_{12}]^{2+}$ was taken as a basis for a rigid potential energy surface (PES) scan of the Ag–Ag distance between 240 to 400 pm at the HF, PBE0, MP2, SCS-MP2, and CCSD(T) levels of theory (Figure 4). The HF rigid PES scan (Ag: cc-pVTZ-PP Se: aug-cc-pVDZ-PP) shows exclusively repulsion for the silver–silver interaction. In contrast, all other employed methods show a shallow minimum in the energy.

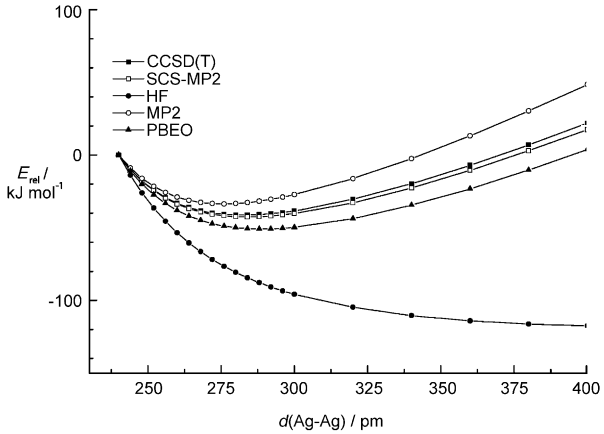

Figure 4. Restricted potential energy surface along the Ag–Ag vector in $[Ag_2Se_{12}]^{2+}$ between 240 and 400 pm at different levels of theory utilizing the basis sets: cc-pVTZ-PP (Ag); aug-cc-pVDZ-PP (Se).

MP2 over estimates[24] the interaction energy with a minimum at an Ag–Ag distance of about 276 pm (cf. solid state structure **2** with 285 pm). Other methods showed minima in interaction energies at 284 pm (SCS-MP2, CCSD(T)) and 288 pm (PBE0) that are in very good agreement with the experimental value. Note that SCS-MP2 shows a well balanced behavior and yielded results comparable to CCSD(T). Therefore, we can deduce that the origin of the by about 40 kJ mol^{-1} attractive Ag–Ag interaction (CCSD(T)) is mainly due to electron-correla-

tion effects. Full details will be disclosed in an upcoming full paper. A simple account for the overall bonding behavior within the $[Ag_2Se_{12}]^{2+}$ cage is offered by the two limiting border cases shown in Figure 5: 1) Complexation: the $[Ag_2Se_{12}]^{2+}$ dication is formed by two silver cations coordinated by a Se_{12} ring, leading to significant Ag–Se bonding; 2) Cluster bonding: the interaction of a hypothetical $[Se_{12}]^{2+}$ cluster with a neutral Ag_2 molecule emphasizes Ag–Ag bonding.

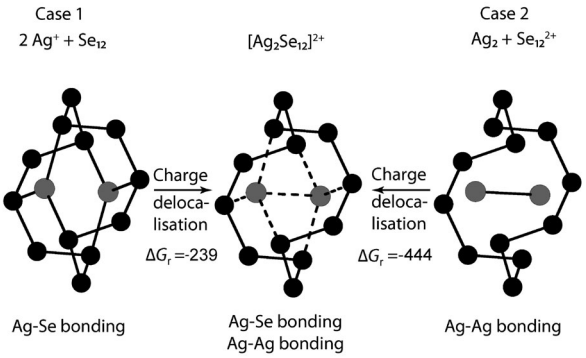

Figure 5. Suggested facile bonding models for the $[Ag_2Se_{12}]^{2+}$ dication. Gibbs energy values [kJ mol^{-1}].

Subsequently, charge delocalization leads to the formation of the $[Ag_2Se_{12}]^{2+}$ cation with intermediate Ag–Se and weak Ag–Ag interactions. The formation of delocalized $[Ag_2Se_{12}]^{2+}$ from these limiting cases is exergonic (PBE0/TZVPP) for both, but the formation of cluster bonding out of complexation is endergonic by 205 kJ mol^{-1}. Thus, the bonding interaction within the $[Ag_2Se_{12}]^{2+}$ structures may be understood as being intermediate between a classical complex and a completely delocalized cluster, slightly favoring complexation.

Received: July 6, 2011
Published online: September 28, 2011

Keywords: ab initio calculations · density functional calculations · metallophilic interactions · selenium · weakly coordinating anions

[1] I. Krossing in *Handbook of Chalcogen Chemistry* (Ed.: F. Devillanova), The Royal Society of Chemistry, Cambridge, **2006**.
[2] D. Aris, J. Beck, A. Decken, I. Dionne, I. Krossing, J. Passmore, E. Rivard, F. Steden, X. Wang, *Phosphorus Sulfur Silicon Relat. Elem.* **2004**, *179*, 859 – 863.
[3] D. Aris, J. Beck, A. Decken, I. Dionne, J. Schmedt auf der Günne, W. Hoffbauer, T. Köchner, I. Krossing, J. Passmore, E. Rivard, F. Steden, X. Wang, *Dalton Trans.* **2011**, 5865 – 5880.
[4] G. Santiso-Quiñones, A. Higelin, J. Schaefer, R. Brückner, C. Knapp, I. Krossing, *Chem. Eur. J.* **2009**, *15*, 6663 – 6677.
[5] H. W. Roesky, M. Thomas, J. Schimlowiak, P. G. Jones, W. Pinkert, G. M. Sheldrick, *J. Chem. Soc. Chem. Commun.* **1982**, 895 – 896; T. S. Cameron, A. Decken, I. Dionne, M. Fang, I. Krossing, J. Passmore, *Chem. Eur. J.* **2002**, *8*, 3386 – 3401.
[6] G. Santiso-Quiñones, R. Brückner, C. Knapp, I. Dionne, J. Passmore, I. Krossing, *Angew. Chem.* **2009**, *121*, 1153 – 1157; *Angew. Chem. Int. Ed.* **2009**, *48*, 1133 – 1137.
[7] a) I. Krossing, A. Reisinger, *Coord. Chem. Rev.* **2006**, *250*, 2721 – 2744; b) I. Krossing, I. Raabe, *Angew. Chem.* **2004**, *116*, 2116 – 2142; *Angew. Chem. Int. Ed.* **2004**, *43*, 2066 – 2090.
[8] M. Wachhold, M. G. Kanatzidis, *J. Am. Chem. Soc.* **1999**, *121*, 4189 – 4195.
[9] M. Wachhold, W. S. Sheldrick, *Z. Naturforsch. B* **1997**, *52*, 169 – 175.
[10] K. Neininger, H. W. Rotter, G. Thiele, *Z. Anorg. Allg. Chem.* **1996**, *622*, 1814 – 1818.
[11] H.-J. Deiseroth, M. Wagener, E. Neumann, *Eur. J. Inorg. Chem.* **2004**, 4755 – 4758.
[12] a) A. Bacchi, W. Baratta, F. Calderazzo, F. Marchetti, G. Pelizzi, *Angew. Chem.* **1994**, *106*, 206 – 207; *Angew. Chem. Int. Ed. Engl.* **1994**, *33*, 193 – 195; b) A. Bacchi, W. Baratta, F. Calderazzo, F. Marchetti, G. Pelizzi, *Inorg. Chem.* **2002**, *41*, 3894 – 3900.
[13] P. Y. Demchenko, R. E. Gladyshevskii, S. V. Volkov, O. G. Yanko, L. B. Kharkova, Z. A. Fokina, A. A. Fokin, *Chem. Commun.* **2010**, *46*, 4520 – 4522.
[14] N. Wiberg, *Holleman Wiberg Lehrbuch der Anorganischen Chemie*, 102 ed., Walther de Gruyter, Berlin, **2007**.
[15] D. R. Lide, *CRC Handbook of Chemistry and Physics*, 83 ed., CRC, Boca Raton, **2002**.
[16] I. Krossing, *Chem. Eur. J.* **2001**, *7*, 490 – 502.
[17] N. Trapp, Dissertation thesis, Albert-Ludwigs Universität (Freiburg), **2008**.
[18] J. Steidel, R. Steudel, A. Kutoglu, *Z. Anorg. Allg. Chem.* **1981**, *476*, 171 – 178.
[19] M. Risto, T. T. Takaluoma, T. Bajorek, R. Oilunkaniemi, R. S. Laitinen, T. Chivers, *Inorg. Chem.* **2009**, *48*, 6271 – 6279.
[20] R. A. Stevens, C. C. Raymond, P. K. Dorhout, *Angew. Chem.* **1995**, *107*, 2737 – 2739; *Angew. Chem. Int. Ed. Engl.* **1995**, *34*, 2509 – 2511.
[21] I. Raabe, K. Wagner, K. Guttsche, M. Wang, M. Grätzel, G. Santiso-Quinones, I. Krossing, *Chem. Eur. J.* **2009**, *15*, 1966 – 1976.
[22] A. Klamt, G. Schüürmann, *J. Chem. Soc. Perkin Trans. 2* **1993**, 799 – 805.
[23] Y. Zhao, D. G. Truhlar, *Acc. Chem. Res.* **2008**, *41*, 157 – 167.
[24] P. Pyykkö, S. Riedel, R. A. Mata, H.-J. Werner, *Chem. Phys. Lett.* **2005**, *405*, 148 – 152; N. Kaltsoyannis, E. O'Grady, *Phys. Chem. Chem. Phys.* **2004**, *6*, 680 – 687.

